Biophysical Journal, Volume *118*

Supplemental Information

Structural Consequences of Multisite Phosphorylation in the BAK1 Kinase Domain

Alexander S. Moffett and Diwakar Shukla

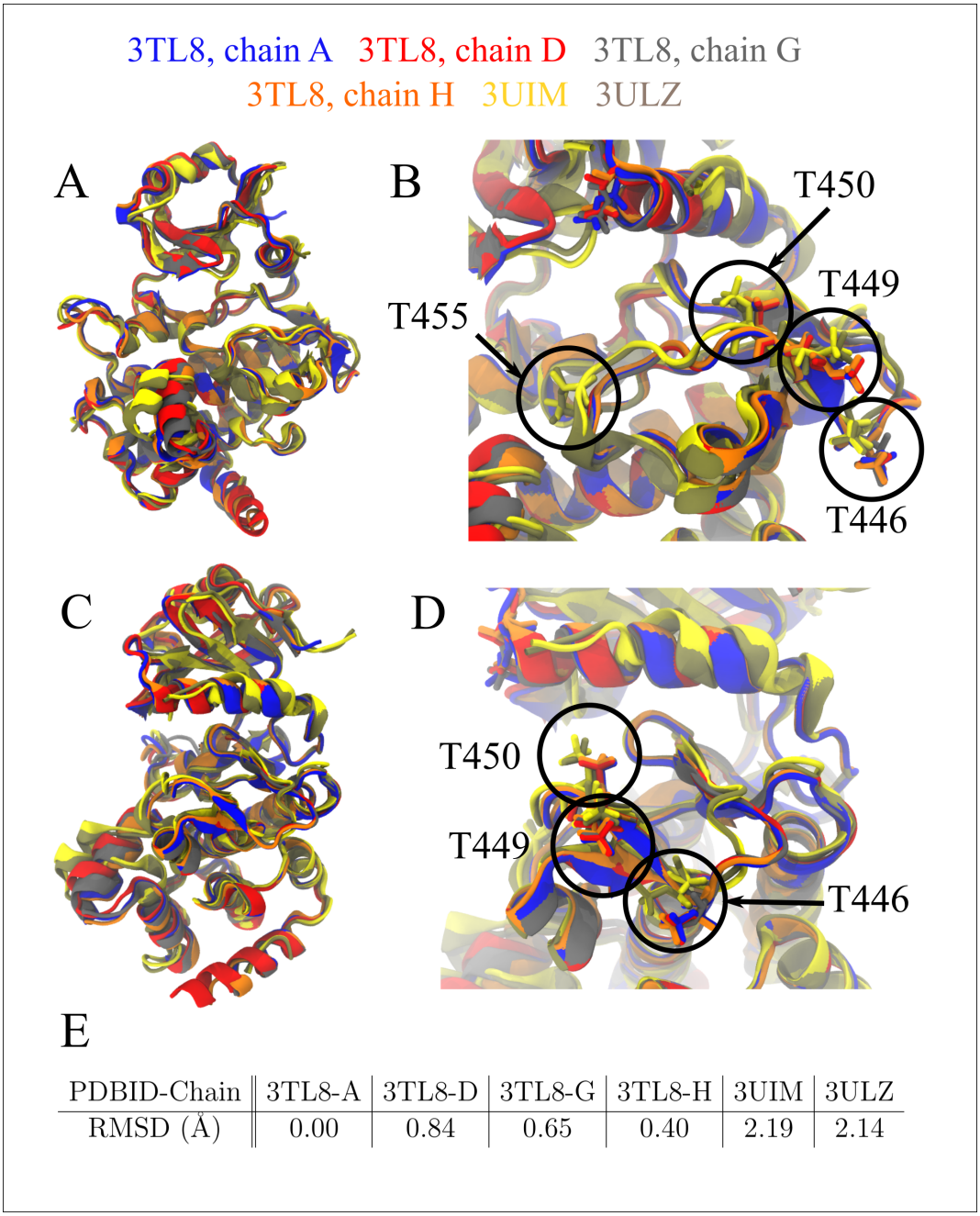

E

PDBID-Chain	3TL8-A	3TL8-D	3TL8-G	3TL8-H	3UIM	3ULZ
RMSD (Å)	0.00	0.84	0.65	0.40	2.19	2.14

Figure S1: Overview of the BAK1 kinase domain crystal structures currently available on the PDB. **A** Structural alignment of all six currently available BAK1 kinase domain crystal structures. Structures were aligned in VMD using MultiSeq. **B** A closeup view of the BAK1 structural alignment, oriented as in **A**. The positions of each activation loop threonine that can be phosphorylated are noted. **C** A view of the BAK1 structural alignment in **A** shown rotated 90° roughly along the principal axis. **D** A closeup of **C**. Note the disorder in the αC helix in PDBID 3UIM and 3ULZ, as well as their subtle difference in activation loop conformation near T446 from the remaining four structures. **E** Backbone RMSD of each crystal structure to PDBID 3TL8 chain A. The backbone atoms in the set of common residues for all six structures was used to align each other structure to 3TL8 chain A and measure the RMSD.

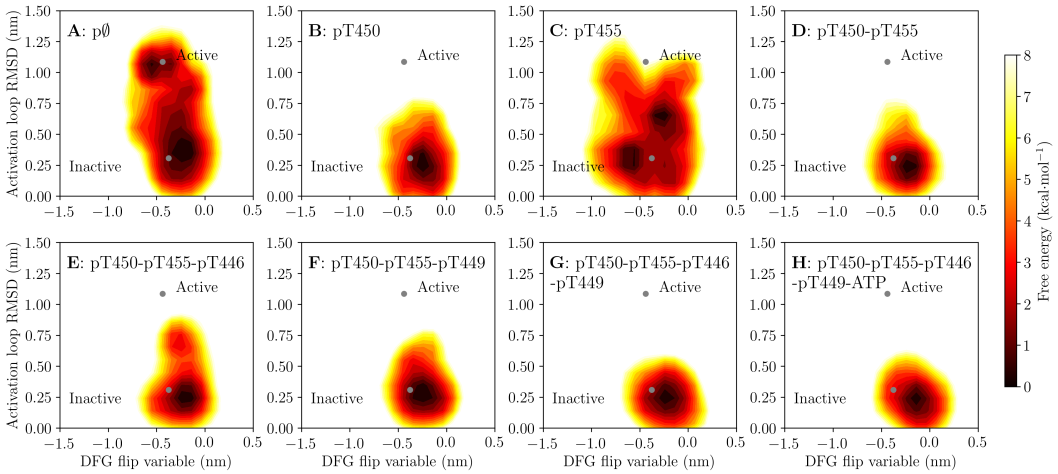

Figure S2: Free energy landscapes over a collective variable describing a DFG flip and the activation loop RMSD as defined in the main text. The DFG flip variable was defined as the distance between L404 α-carbon and C4 of the F435 side chain minus the distance between D416 α-carbon and C4 of the F435 side chain. The notation pØ is used as shorthand for the unphosphorylated BAK1 kinase domain. The PMFs were calculated from GAMD simulations reweighted using MBAR.

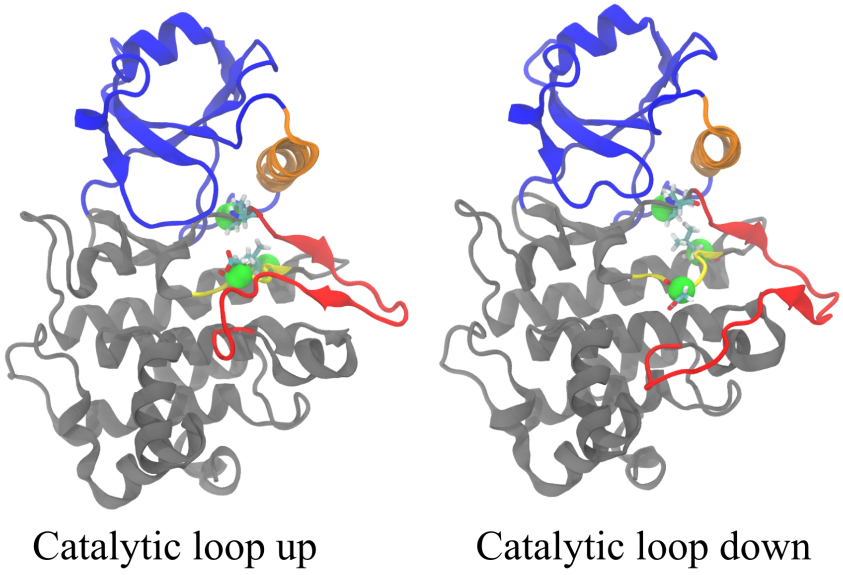

Figure S3: Flip of the catalytic loop in BAK1 away from the active site, resulting in a greater distance between D416 and F435.

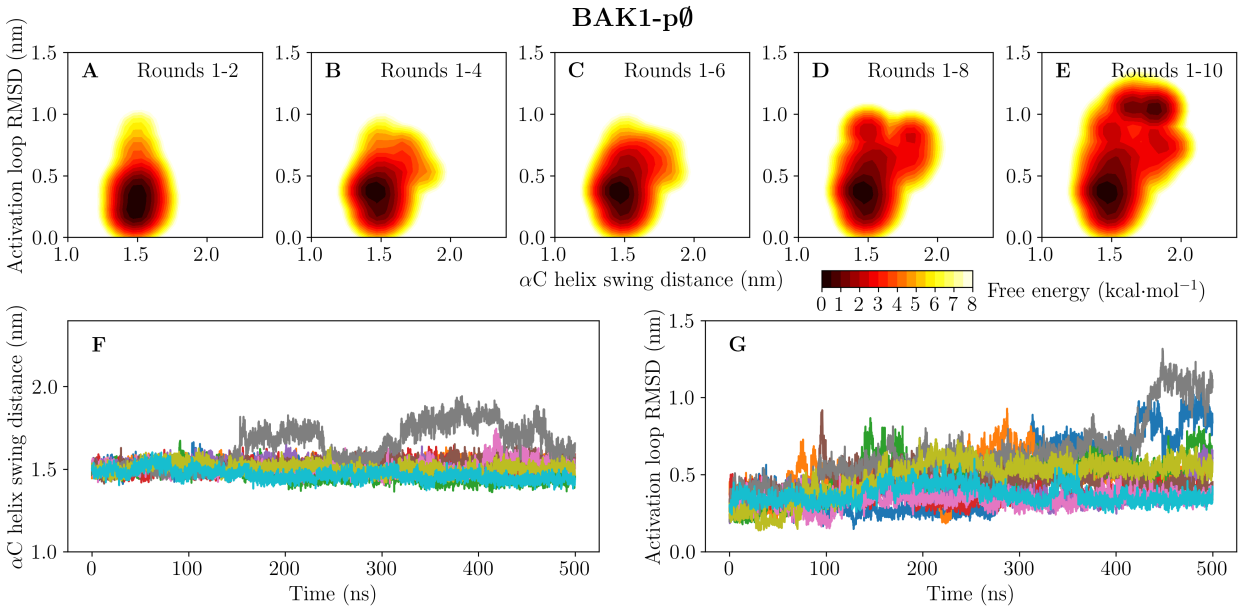

Figure S4: **A-E** Two-dimensional PMFs over the activation loop RMSD to a crystal structure (3TL8, chain A) and the αC helix swing distance with progressively more sampling used. **F** The αC helix swing distance with time for each of the 10 replicate GAMD simulations. **G** The activation loop RMSD with time for each of the 10 replicate GAMD simulations.

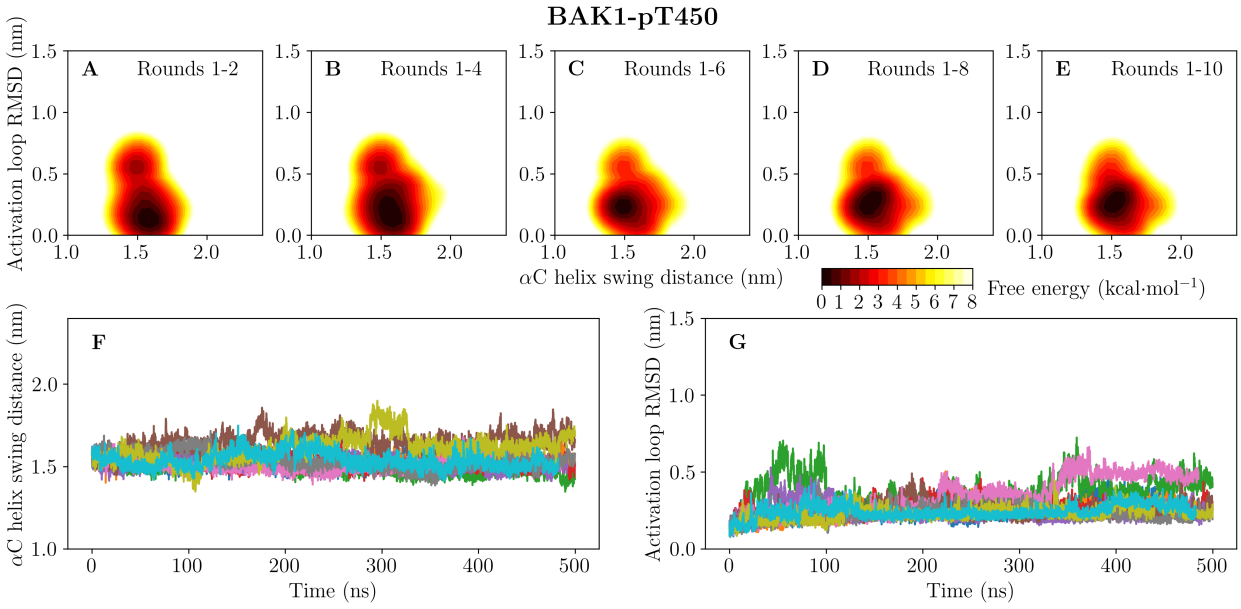

Figure S5: **A-E** Two-dimensional PMFs over the activation loop RMSD to a crystal structure (3TL8, chain A) and the αC helix swing distance with progressively more sampling used. **F** The αC helix swing distance with time for each of the 10 replicate GAMD simulations. **G** The activation loop RMSD with time for each of the 10 replicate GAMD simulations.

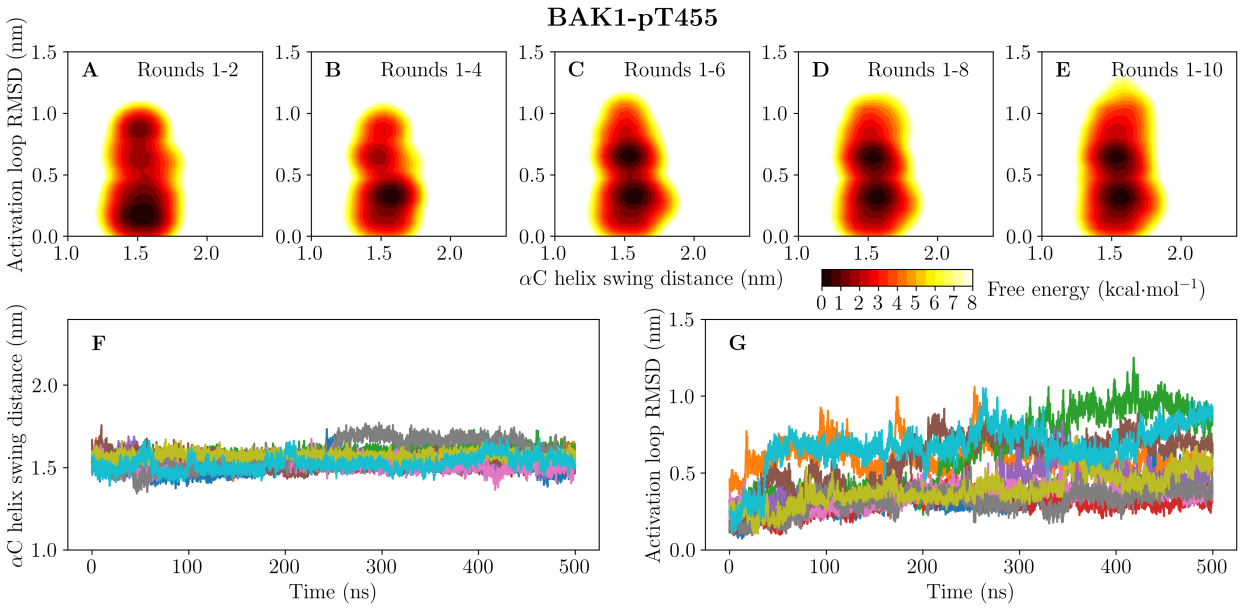

Figure S6: **A-E** Two-dimensional PMFs over the activation loop RMSD to a crystal structure (3TL8, chain A) and the αC helix swing distance with progressively more sampling used. **F** The αC helix swing distance with time for each of the 10 replicate GAMD simulations. **G** The activation loop RMSD with time for each of the 10 replicate GAMD simulations.

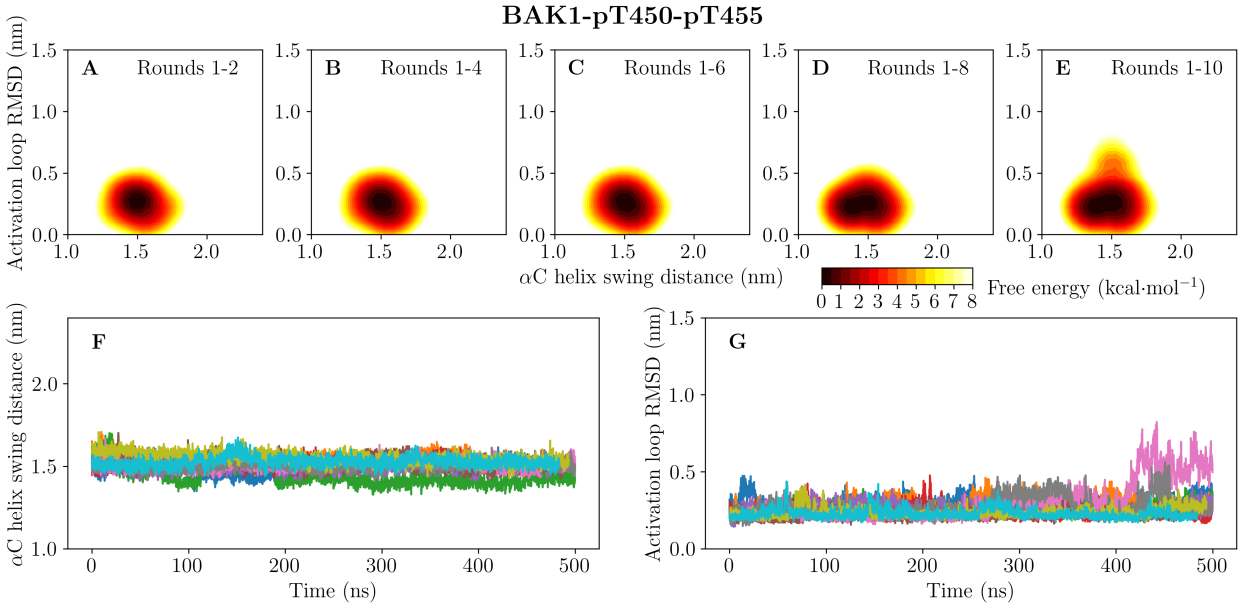

Figure S7: **A-E** Two-dimensional PMFs over the activation loop RMSD to a crystal structure (3TL8, chain A) and the αC helix swing distance with progressively more sampling used. **F** The αC helix swing distance with time for each of the 10 replicate GAMD simulations. **G** The activation loop RMSD with time for each of the 10 replicate GAMD simulations.

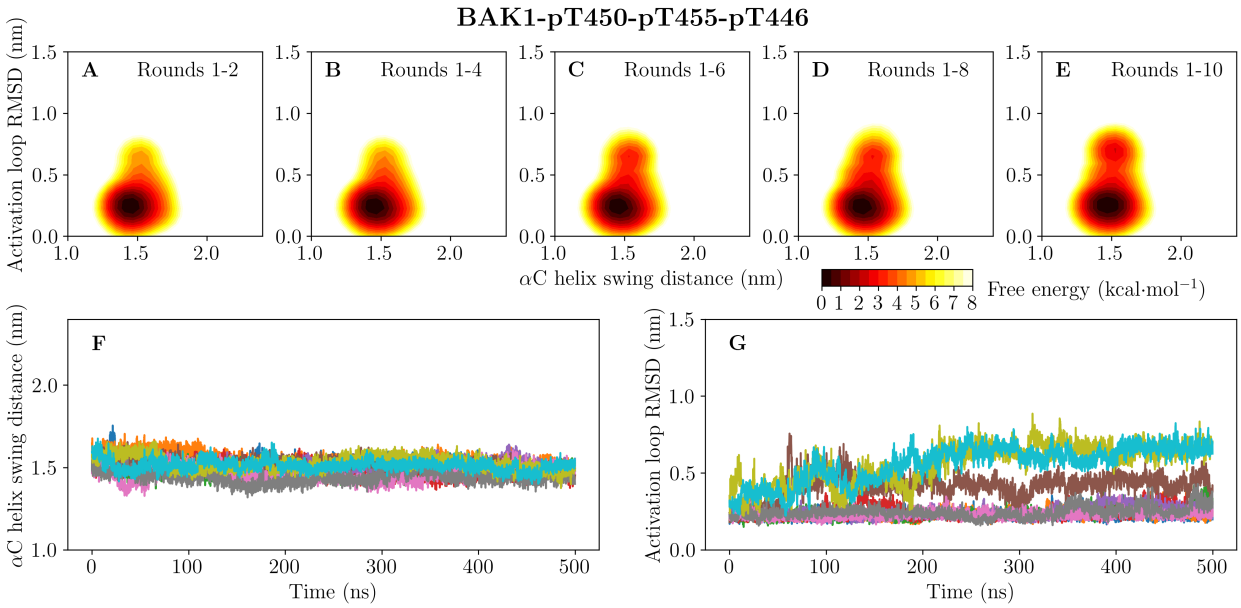

Figure S8: **A-E** Two-dimensional PMFs over the activation loop RMSD to a crystal structure (3TL8, chain A) and the αC helix swing distance with progressively more sampling used. **F** The αC helix swing distance with time for each of the 10 replicate GAMD simulations. **G** The activation loop RMSD with time for each of the 10 replicate GAMD simulations.

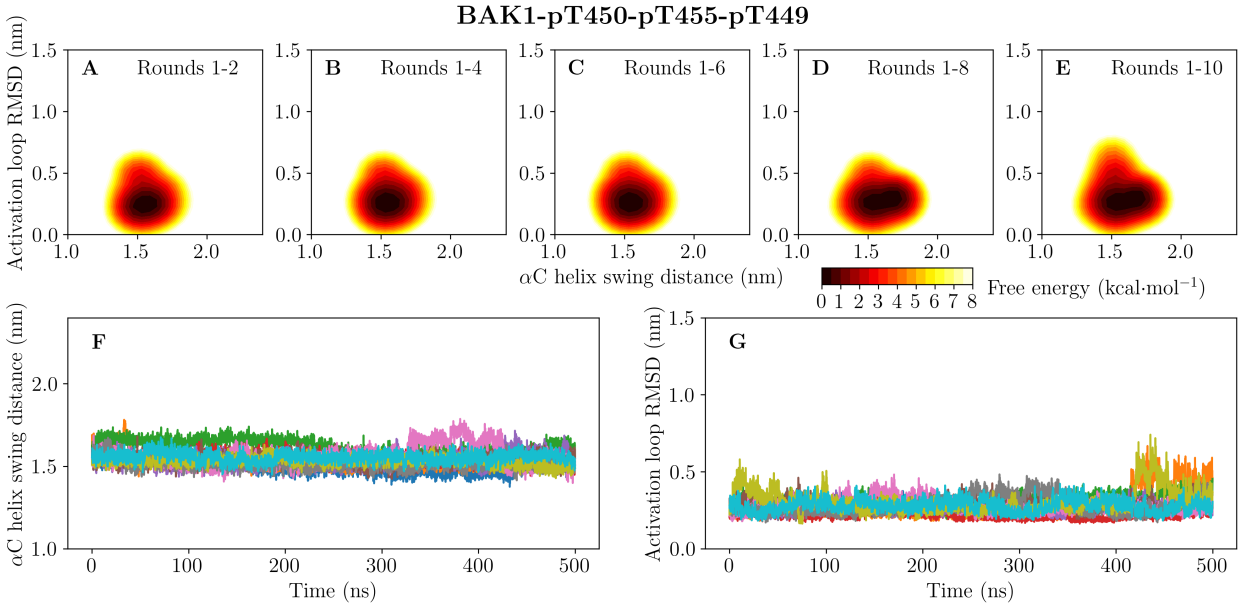

Figure S9: **A-E** Two-dimensional PMFs over the activation loop RMSD to a crystal structure (3TL8, chain A) and the αC helix swing distance with progressively more sampling used. **F** The αC helix swing distance with time for each of the 10 replicate GAMD simulations. **G** The activation loop RMSD with time for each of the 10 replicate GAMD simulations.

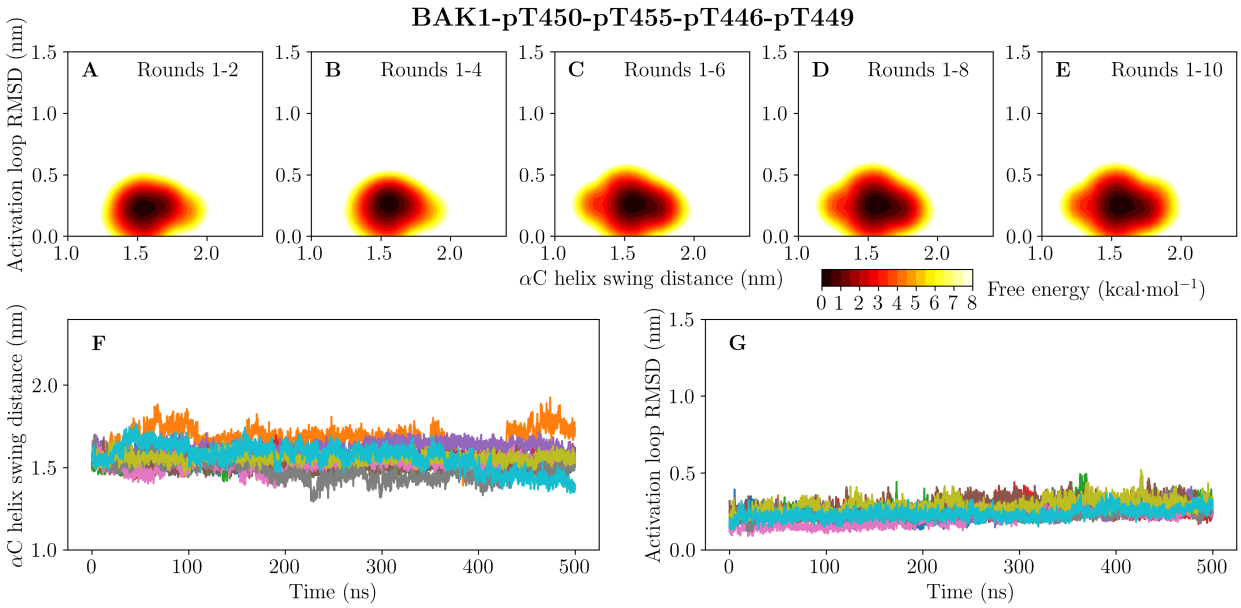

Figure S10: **A-E** Two-dimensional PMFs over the activation loop RMSD to a crystal structure (3TL8, chain A) and the αC helix swing distance with progressively more sampling used. **F** The αC helix swing distance with time for each of the 10 replicate GAMD simulations. **G** The activation loop RMSD with time for each of the 10 replicate GAMD simulations.

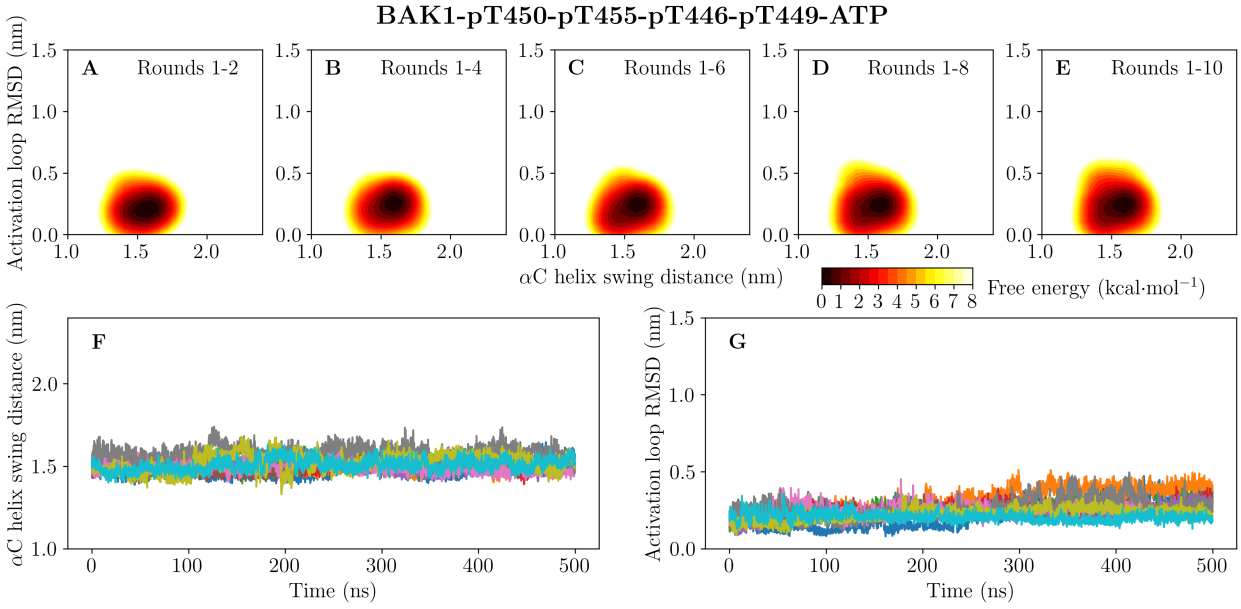

Figure S11: **A-E** Two-dimensional PMFs over the activation loop RMSD to a crystal structure (3TL8, chain A) and the αC helix swing distance with progressively more sampling used. **F** The αC helix swing distance with time for each of the 10 replicate GAMD simulations. **G** The activation loop RMSD with time for each of the 10 replicate GAMD simulations.

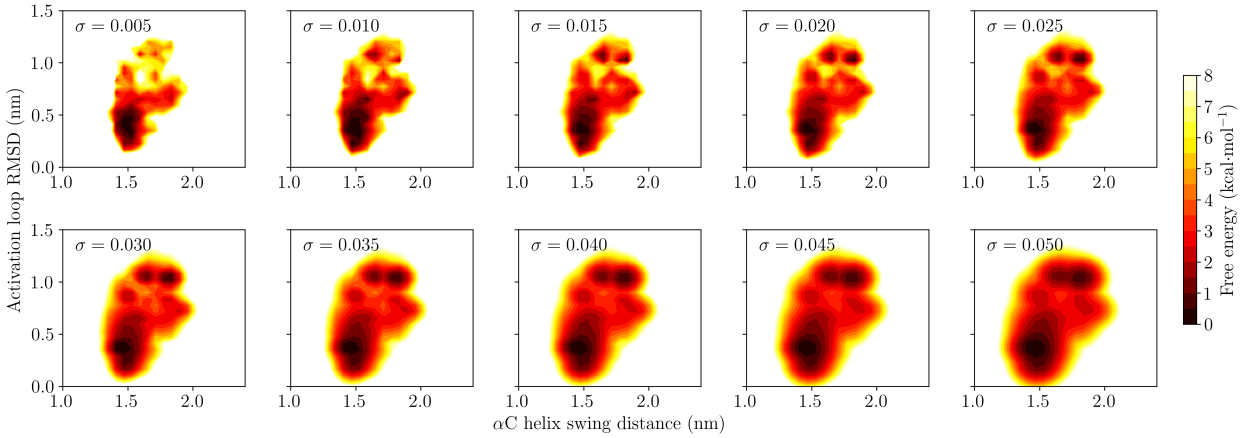

Figure S12: Two-dimensional PMFs of unphosphorylated BAK1 over the activation loop RMSD to a crystal structure (3TL8, chain A) and the αC helix swing distance, with the Gaussian basis function bandwidth varying from 0.005 nm to 0.05 nm.

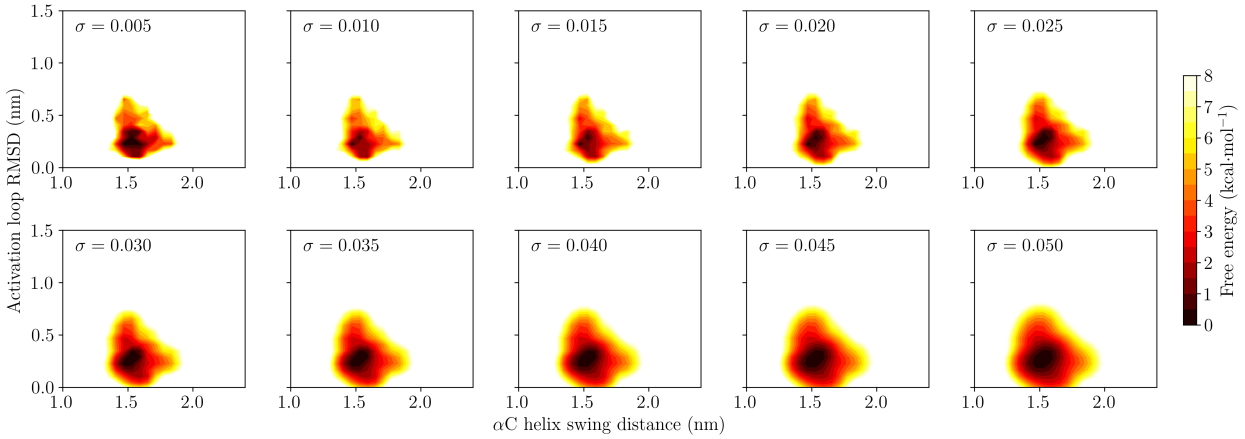

Figure S13: Two-dimensional PMFs of BAK1 pT450 over the activation loop RMSD to a crystal structure (3TL8, chain A) and the αC helix swing distance, with the Gaussian basis function bandwidth varying from 0.005 nm to 0.05 nm.

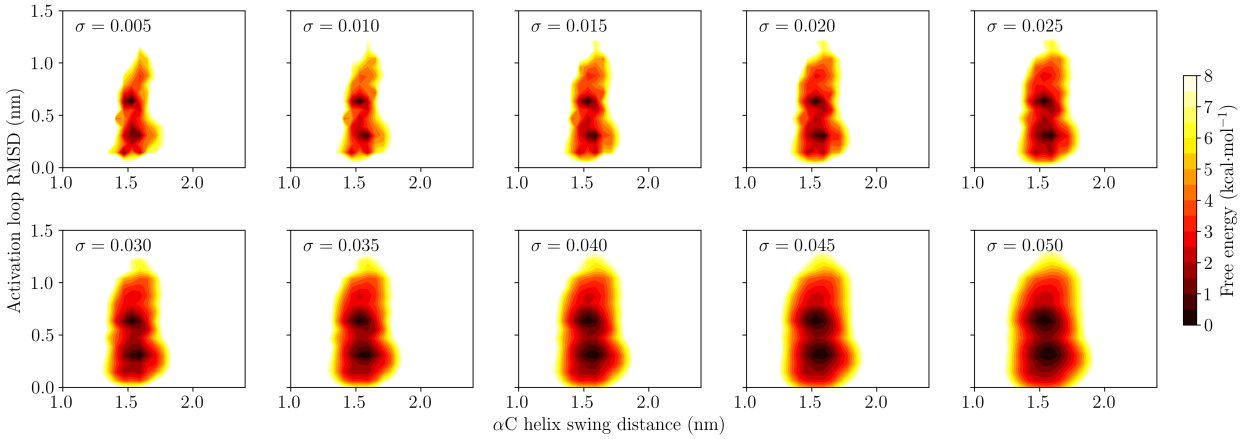

Figure S14: Two-dimensional PMFs of BAK1 pT455 over the activation loop RMSD to a crystal structure (3TL8, chain A) and the αC helix swing distance, with the Gaussian basis function bandwidth varying from 0.005 nm to 0.05 nm.

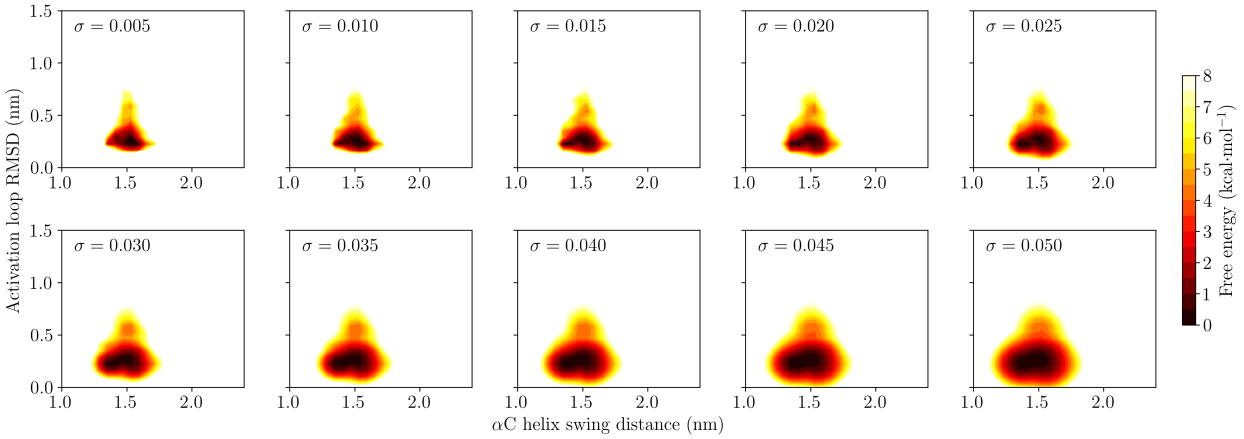

Figure S15: Two-dimensional PMFs of BAK1 pT450-pT455 over the activation loop RMSD to a crystal structure (3TL8, chain A) and the αC helix swing distance, with the Gaussian basis function bandwidth varying from 0.005 nm to 0.05 nm.

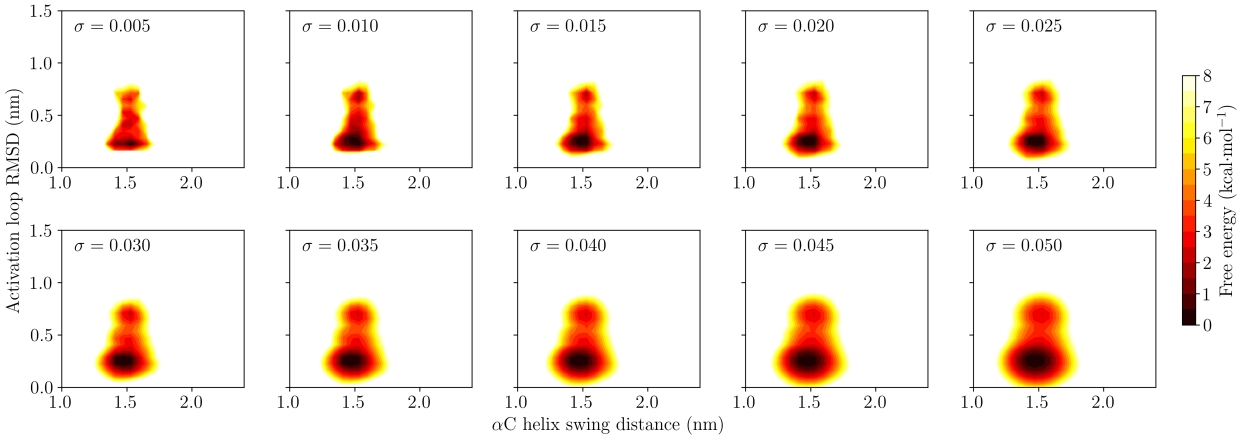

Figure S16: Two-dimensional PMFs of BAK1 pT446-pT450-pT455 over the activation loop RMSD to a crystal structure (3TL8, chain A) and the αC helix swing distance, with the Gaussian basis function bandwidth varying from 0.005 nm to 0.05 nm.

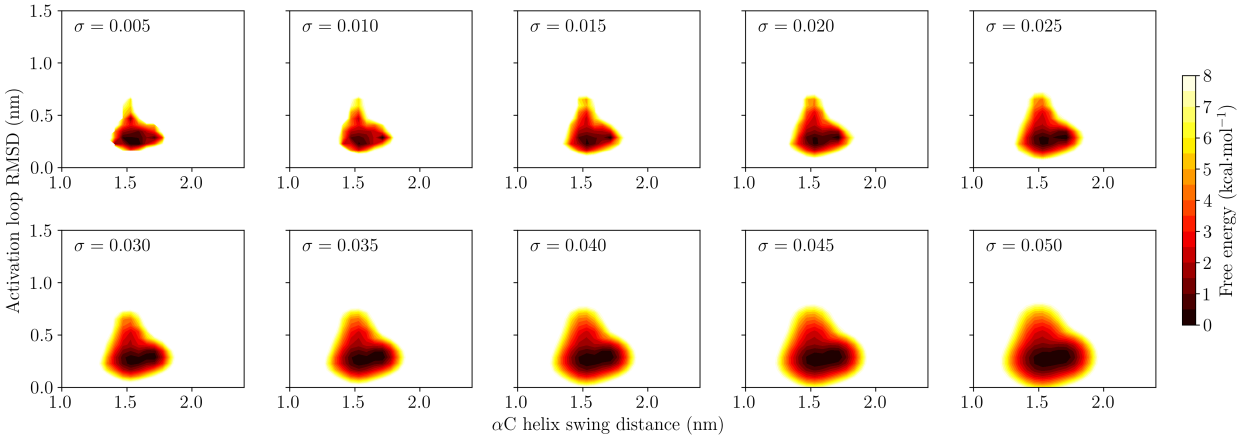

Figure S17: Two-dimensional PMFs of BAK1 pT449-pT450-pT455 over the activation loop RMSD to a crystal structure (3TL8, chain A) and the αC helix swing distance, with the Gaussian basis function bandwidth varying from 0.005 nm to 0.05 nm.

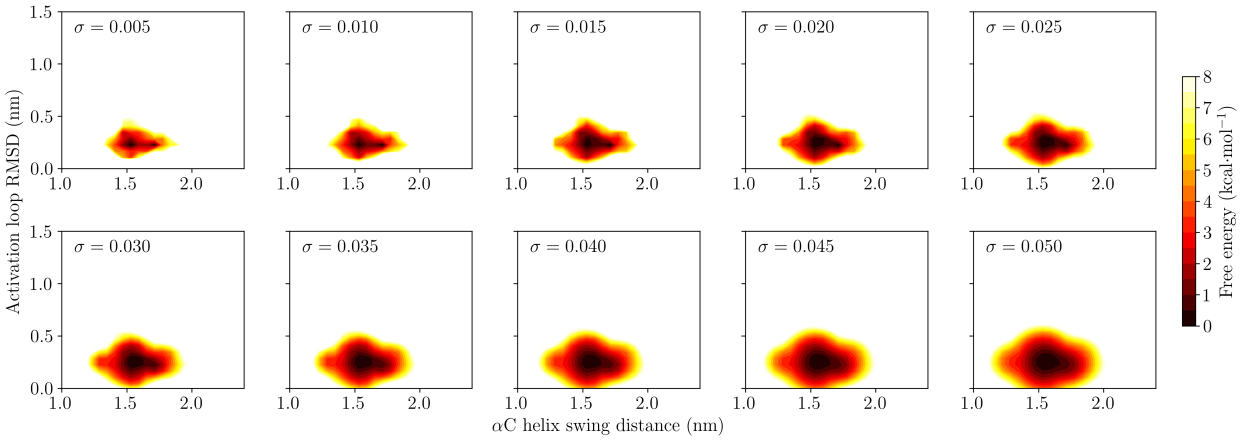

Figure S18: Two-dimensional PMFs of BAK1 pT446-pT449-pT450-pT455 over the activation loop RMSD to a crystal structure (3TL8, chain A) and the αC helix swing distance, with the Gaussian basis function bandwidth varying from 0.005 nm to 0.05 nm.

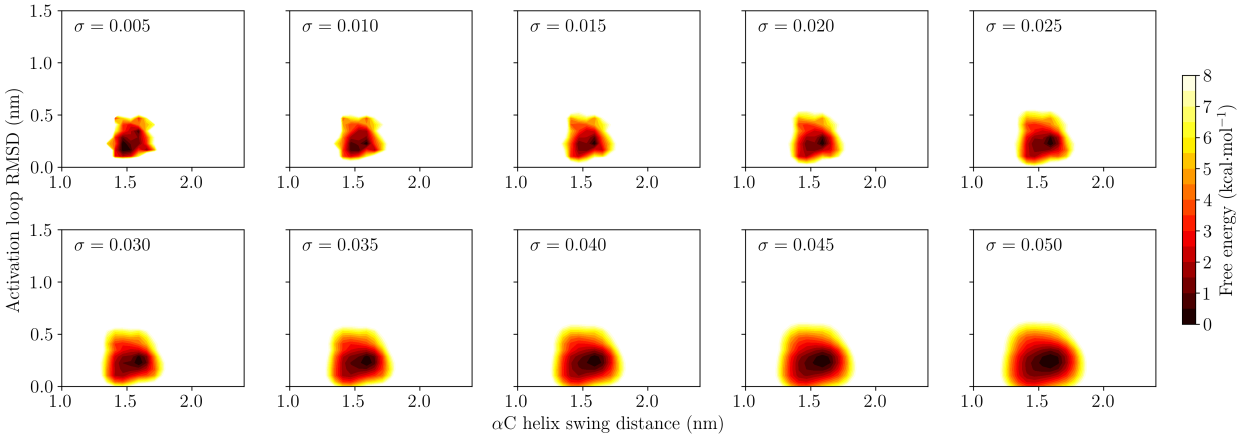

Figure S19: Two-dimensional PMFs of ATP-bound BAK1 pT446-pT449-pT450-pT455 over the activation loop RMSD to a crystal structure (3TL8, chain A) and the αC helix swing distance, with the Gaussian basis function bandwidth varying from 0.005 nm to 0.05 nm.

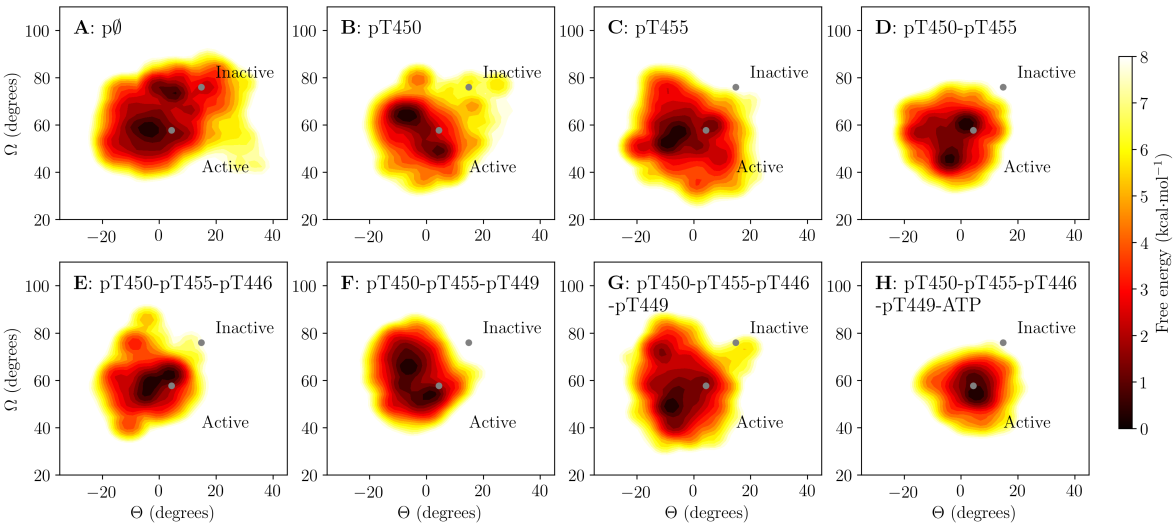

Figure S20: PMFs over the BAK1 inter-lobe angles Ω and Θ. The notation pØ is used as shorthand for the unphosphorylated BAK1 kinase domain. The PMFs were calculated from GAMD simulations reweighted using MBAR.

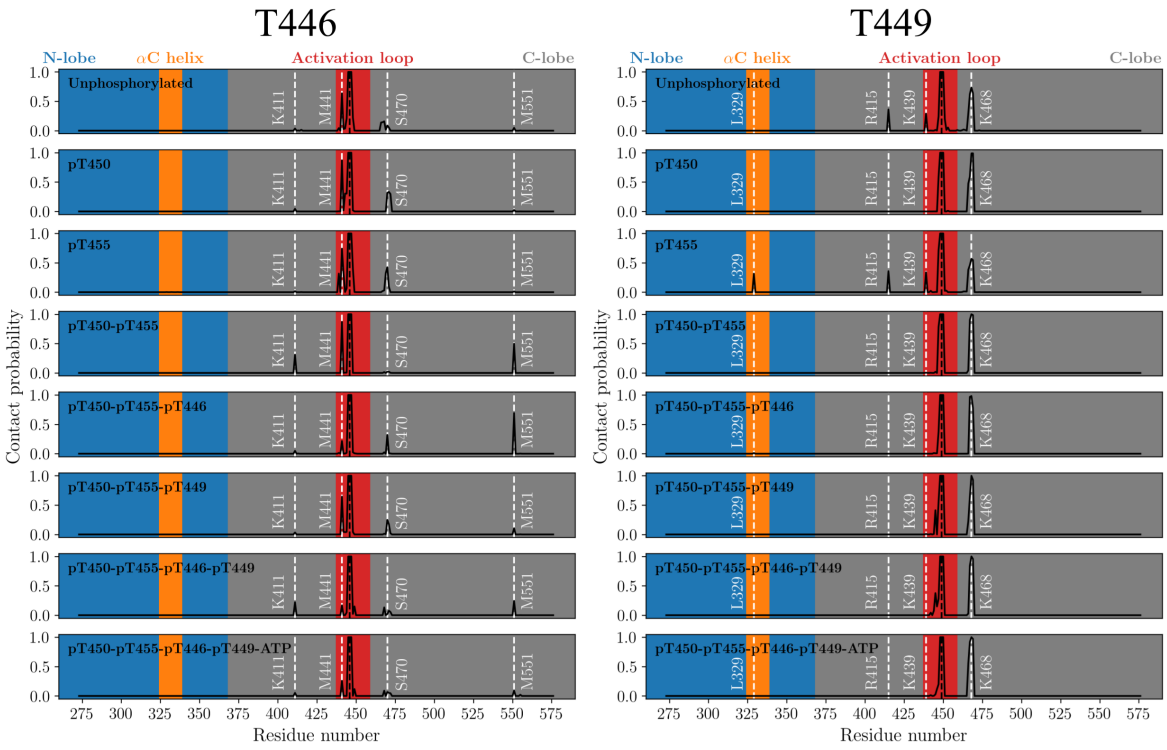

Figure S21: Contact probabilities for BAK1 T446 and T449 in each mod-form, reweighted using MBAR. The black dotted lines represent the reference threonine residue, while white dotted lines denote contacting residues of interest.

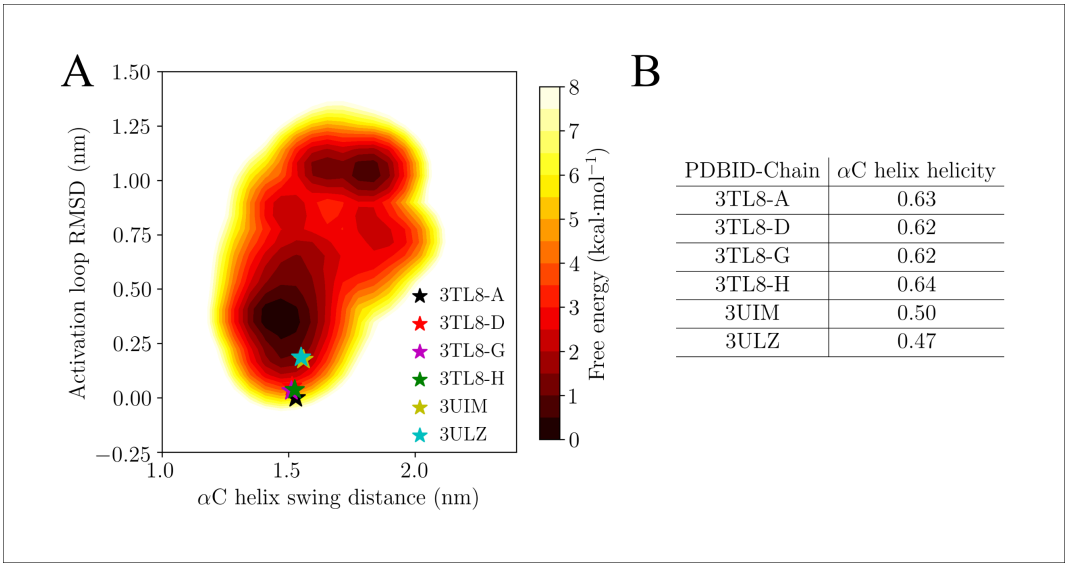

PDBID-Chain	αC helix helicity
3TL8-A	0.63
3TL8-D	0.62
3TL8-G	0.62
3TL8-H	0.64
3UIM	0.50
3ULZ	0.47

Figure S22: **A** The two-dimensional PMF of unphosphorylated BAK1 over the activation loop RMSD to a crystal structure (3TL8, chain A) and the αC helix swing distance, with the the location of each crystal structure on the landscape indicated. Analysis was performed on the set of common residues for all six structures. **B** The helicity of the αC helix in all currently available BAK1 kinase domain crystal structures. For this measurement as well, analysis was performed on the set of common residues for all six structures.